Plant Physiol. (1974) 53, 47–51

A Digital Diffusion Porometer Circuit[1]

Received for publication March 19, 1973 and in revised form September 4, 1973

EDWIN L. FISCUS
Department of Botany, Duke University, Durham, North Carolina 27706

ABSTRACT

An automatic digital diffusion porometer circuit is described. The circuit is highly stable with respect to temperature and supply voltage. The device is capable of high timing accuracy over very short measurement intervals, so that measurements may be made rapidly without the danger of stomatal changes occurring during the measurement period.

Stomatal resistance as an indicator of the relative degree of plant water stress is receiving wide acceptance. Attempts to measure stomatal opening have led to the development of a wide variety of portable instruments ranging from the pressure flow porometer of Alvim (1) to the electromechanical device described by Kenny and McGruddy (3). Instruments commercially available at this time are modeled after the one described by Kanemasu *et al.* (2). Stomatal resistance is determined with this type of instrument by measuring the time rate of voltage change (dV/dt) across a humidity-sensitive resistor. The time necessary for the circuit output to traverse two arbitrary points on the output meter scale is generally determined with a stopwatch or an electromechanical counter (3). The dV/dt characteristics are related to diffusion resistance through calibration of the instrument with a series of standard diffusion barriers.

In addition to the operational difficulties and timing errors discussed by Kenny and McGruddy (3), another potential source of error is due to changes in the stomata during a measurement period. It is therefore desirable to obtain the resistance measurement as soon after placing the sensor on the leaf as possible. Conventional instruments are limited in this respect by the meter movement delicacy and response time as well as timing accuracy. This paper describes a portable solid state automatic porometer timing circuit with a crystal controlled time base and independently variable set points. This instrument is lightweight (1.6 kg), stable, easy to operate, and has high timing accuracy over very short (0–3 sec) measurement intervals.

MATERIALS AND METHODS

The circuit was designed to operate with the standard humidity and temperature sensors available from Lambda Instruments, Inc. (2933 N. 36th St., Lincoln, Neb.). It seemed desirable to design our circuit in such a way that it was as nearly compatible with the commercial instrument as possible. The output of the available instruments is a nonlinear d.c. ramp of approximately 50 mv peak. The circuit was designed from this starting point. Briefly, the ramp is amplified and fed into the control circuit which senses the elapsed time between two set points. This elapsed time appears as a four-digit numerical readout. Proper manipulation of the amplifier and control circuit allows adjustment of the set points over the entire range of the humidity sensor. The circuit details and operational description are given in the "Appendix."

The sensor (Lambda Instruments Model LI-15S) was calibrated on a laboratory benchtop using the standard calibration plate supplied by Lambda. Initial calibrations were made at different temperatures, and portions of the calibrations were repeated at various time intervals. Figure 1 shows a typical calibration curve made over a period of 3 days, 1 day at each temperature. Calibration at the highest temperature was then repeated on two successive days, while the intermediate temperature was repeated after an interval of 2 months.

Linear regressions were performed on all sets of data. The resulting equations were used to generate data concerning the relationship between regression constants and temperature. These data were subjected to regression analysis, and the two resultant equations were used to predict the curves for temperatures which were not actually calibrated. In addition, these predicted values were compared with the observed values of the initial and replicated calibrations.

The digital circuit was also compared with a standard Lambda Instruments device. The comparative measurements were made simultaneously by coupling the output of the analog porometer to the input of the digital device so that both instruments were operating from a single sensor. Thus, a point-for-point comparison of the two timing methods was possible. The timing intervals used for the digital device were made much smaller for the comparative test than for normal (Fig. 1) operation in an attempt to maximize any discrepancies between the two methods. The comparative tests were also carried out with the calibration plate supplied by Lambda. This method was thought to yield a far more accurate comparison than any other approach.

RESULTS AND DISCUSSION

A typical calibration appears in Figure 1. The slopes and intercepts of the lines show the typical negative temperature coefficients. Over the temperature range shown, these coefficients may be approximated by a linear model. Linear regression constants were used to calculate the slopes and intercepts of all the calibration lines, and these predicted values are compared with the observed values in Table I. The important point to consider in Table I, with reference to stability and reproducibility, is not the absolute size of the difference between the observed and predicted values at any one temperature. It is important rather to compare the size of the difference between

[1] This work was supported by National Science Foundation Grant GB-30367X.

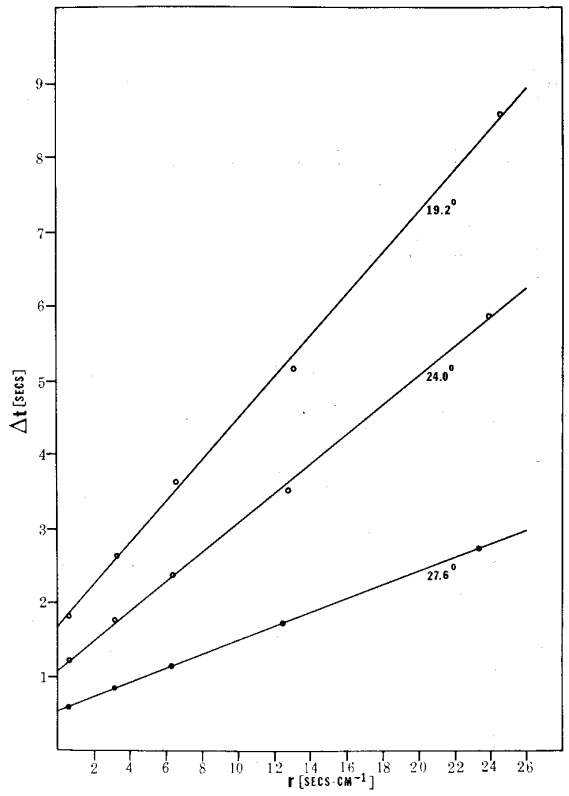

FIG. 1. Typical calibration showing sensor temperature variation.

replicates at or near the same temperature. Table I shows that the instrument possesses excellent short and long term stability and that calibration curves are quite readily reproduced.

Although the temperature coefficients for slope and intercept may be linearly approximated over the temperature range shown, its over-all nonlinearity becomes apparent when the temperature range is extended.

The results of the comparison between the two timing methods are shown in Figure 2. A linear regression was performed on the raw data. The points on the line are average values for each cluster. It is apparent from the figure that a good linear relationship exists between the two methods, even when the automatically determined time periods were very small. Since disagreement between the methods should have been at its greatest with the very small time intervals used in the comparison, we feel that Figure 2 demonstrates very good agreement between the two methods.

It should be pointed out that the usual diffusion porometer operating precautions become somewhat more stringent as the timing period is decreased. It is therefore important, as it is with any diffusion porometer, that the sensor be properly dried, and the chamber walls be equilibrated near the operating point. Since excursions from the initial set point are kept small in the digital device during operation, this condition is easily maintained. A rule of thumb which we have found useful in calibration of the instrument, which presumably holds true for experimental determinations as well, is that the sensor is ready for use when the rate of water desorption from the sensor and chamber walls and external leakage is at least 10 times longer than the longest measurement interval.

The only significant drawback to the circuit which we can ascertain is the low visibility of the readout under high ambient light conditions. This problem is easily remedied during construction by shielding the display with a hood.

Inasmuch as the electronic measurement time could be made a small fraction of the manual method and showed good agreement with it and in view of the reproducible behavior of the instrument, we feel that the use of the instrument is justified. Elimination of the burden of manual timing and the use of shorter timing periods makes the porometer considerably faster and easier to use. It also is more accurate, both because of the precision time base and because the shorter period required for measurement decreases the danger of causing abnormal changes in stomatal aperture.

APPENDIX

The complete circuit consists of six distinct subsections which are detailed in Figures 3 through 7 and will be described separately.

The ramp generated by the hygrometer circuit is fed into the noninverting operational amplifier (IC-1) with a nominal gain of 100 (Fig. 3). The output is buffered by the voltage follower Q_1 and fed into the set point and gating circuitry.

The set point circuit consists of two identical stages which take advantage of the negative resistance characteristics of the unijunction transistors (UJT) Q_2 and Q_4.

Table I. *Comparison of Initial and Replicated Calibration Curves*

Predicted values were obtained by regression of slopes and intercepts on temperature for all calibrations.

	Temperature (C)					
	19.2	24.0	23.8[1]	27.6	27.4[2]	27.6[2]
Slope						
Predicted	0.306	0.186	0.191	0.096	0.101	0.096
Observed	0.297	0.197	0.207	0.093	0.104	0.089
Difference	−0.009	0.011	0.016	−0.003	0.003	−0.007
Intercept						
Predicted	1.70	1.03	1.05	0.52	0.55	0.52
Observed	1.68	1.09	1.05	0.54	0.49	0.52
Difference	−0.02	0.06	0.00	0.02	−0.06	0.00

[1] Long term replications.
[2] Short term replications.

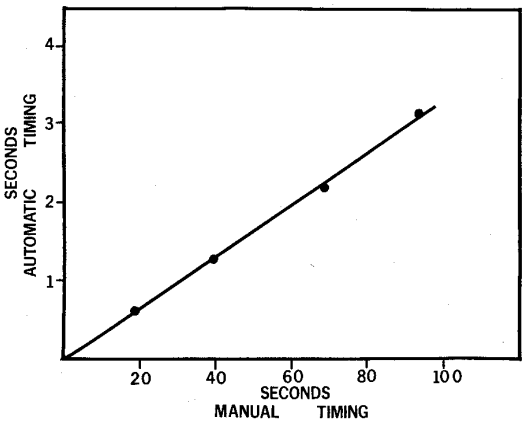

FIG. 2. Comparison of automatic and manual timing methods. r: 0.975; b: −0.038; m: 0.033 with df = 73.

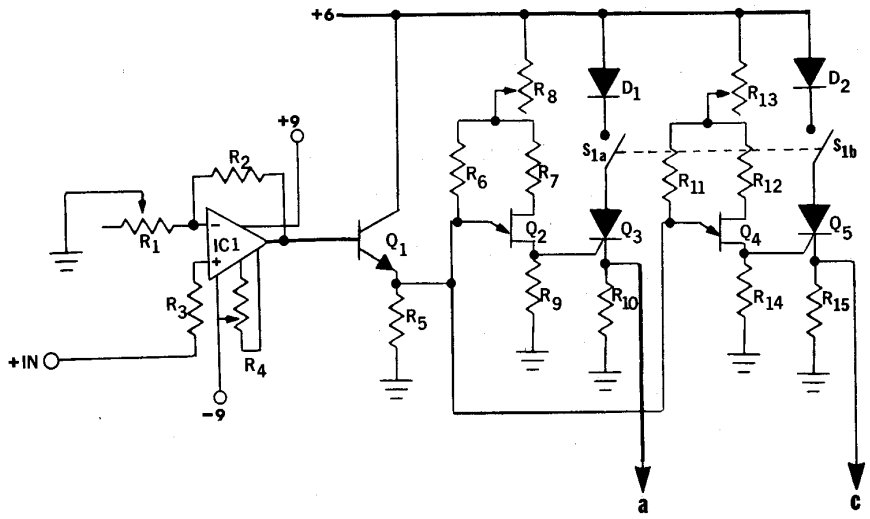

FIG. 3. Input ramp amplifier and set point circuit.

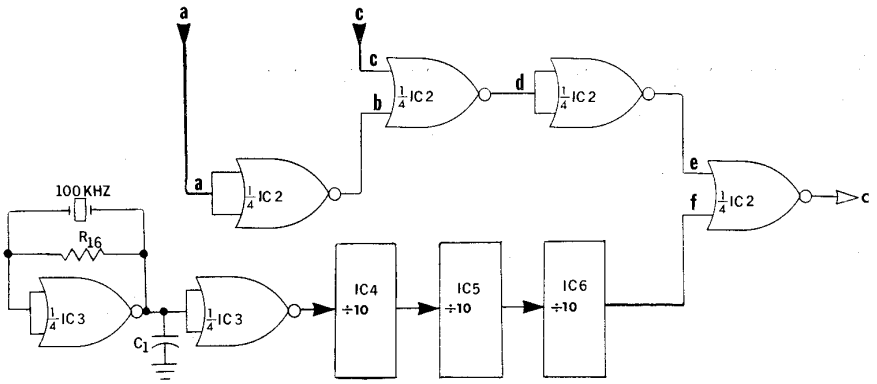

FIG. 4. Crystal time base and control logic.

The peak point emitter voltage (V_p) for these devices can be written as[2]

$$V_p = V_d + \eta V_{b2b1} \quad (1)$$

where V_d is the emitter-base 2 diode forward voltage drop, η is the intrinsic standoff ratio, and V_{b2b1} is the voltage imposed across base 2 and base 1. It is clear from equation 1 that V_p can be varied by manipulating V_{b2b1}. This is done by dropping the supply voltage through potentiometers R_8 and R_{13}. In this way, it is possible to vary V_p for each stage independently of the other. It is therefore possible to set the control points arbitrarily close together. The actual control signals are taken from silicon-controlled rectifier (SCR) stages Q_3 and Q_5 which follow the UJT control points. The control signals appear at points a and c of Figures 3 and 4. Figure 4 illustrates the proper sequencing and control functions of the control gates during a measurement period. A high signal at e inhibits the incoming clock signal at f, which is gated through to the counting units only when e is low. The gating up to point e operates as a logical "exclusive nor" gate if, and only if, the signal at a goes high before c. This is necessary to the functioning of the whole system and is easy to arrange since the set points are independently variable.

A 100 Hz clock signal is provided by a 100 kHz crystal-controlled nor gate oscillator. The primary frequency is divided by three decade scalers (ICs, 4, 5, and 6) and fed to the final control gate at point f. This last gate also buffers the clock signal which then goes to the counting circuitry when the input to e is low. In addition, the 1 kHz output from IC-5 is tapped to excite the hygrometer circuit.

The four serially arranged CD4033A devices (Fig. 5) count the clock pulses when e is low and provide a decoded seven-segment output. The decoded output is buffered by the CA3082 transister arrays which control the current to the seven-segment incandescent displays. Only one set of buffers and displays is shown.

Power is conserved by blanking the displays until the completion of a measurement cycle. Depression of the "display enable" switch actuates the display. Additional power conservation is achieved through use of the "ripple blanking" function of the CD4033A devices[3] and the use of 74L series decade scalers. The ripple blanking function allows for blanking of the leading and trailing zeros in the display.

[2] Motorola. 1971. Theory and characteristics of the unijunction transistor. Application Note AN-293, Motorola Semiconductor Products, Inc., Phoenix, Ariz.

[3] RCA. 1972. COS/MOS ICs for low voltage applications. File No. 503. RCA Solid State Division, Somerville, N.J. (2).

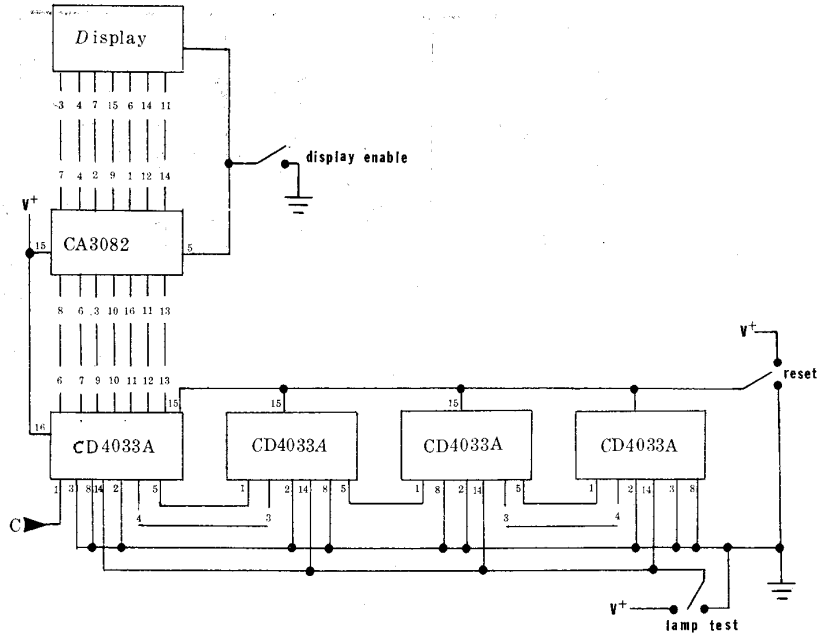

FIG. 5. Pulse counting and display circuit. Interfacing of the four serial counting units is shown but only one set of buffers and displays are illustrated.

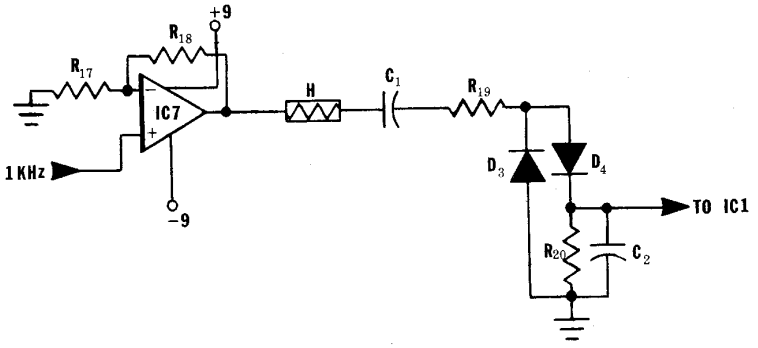

FIG. 6. Hygrometer circuit.

The hygrometer circuit (Fig. 6) is a conventional type (2, 3). It is actuated by a 1 kHz clock signal amplified 1.5 times by IC-7 putting a nominal 7.5 v square wave across the circuit. The circuit output is then rectified and filtered before going to IC-1 and the set point circuitry.

The temperature circuit (Fig. 7) consists of a single IC timer[4] connected in a monostable configuration. The output pulse period is initiated by the pushbutton switch and programmed by C_3 and the thermistor T. The monostable output is connected to the logic circuit at point d, so that when d goes high, the clock signal is gated to the CD4033A counting units for the duration of the timing pulse. Although the temperature circuit is simple, it yields a count inversely proportional to the temperature and must be read from a calibration chart or equation.

Set Point Adjustment. Although V_p is a linear function of V_{b2b1}, due to the circuit configuration, the relationship between the set point potentiometers (Rs) and the actual UJT firing points as seen from the input, is highly nonlinear. Operation with 1K $<$ Rs $<$ 5K allows more precise control of the set points but over a smaller range than with Rs $<$ 1K. This relationship is highly device-dependent and care should be exercised in substituting the UJTs.

Set Point Stability. As pointed out earlier V_p is subject to supply voltage variations. V_p is also affected by temperature. This circuit was designed to maximize temperature stability by proper selection of the base 2 resistor. In the case of both supply and temperature variations, the absolute set points will shift, but the relationship between the two points will remain constant, since both are subjected to the same variations. Temperature and supply problems therefore are negligible.

Temperature Circuit Stability. The IC timer, which forms the heart of the temperature measuring circuit, has a very small temperature coefficient (0.0005%/C), and the pulse period is independent of supply voltage so that no adjustments to this circuit are necessary.

Power Supply. Both operational amplifiers are powered by one pair of ordinary 9-v transistor batteries. One other 6-v dry cell is used to power all the other circuitry directly except for the decade scalers. In this case, the supply voltage is dropped through a 500 ohm potentiometer to 5 v. Proper supply voltage to the scalers is indicated simply by their

[4] Signetics. 1972. Timer/555. Signetics, Sunnyvale, Calif. (3).

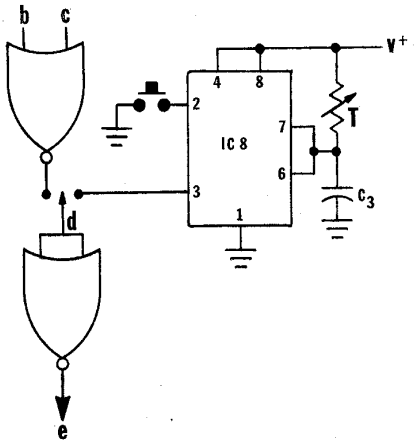

FIG. 7. Temperature measuring circuit and interfacing with control logic.

operation so that the adjustment is made quite easily in the field. We have, in any case, rarely found this adjustment necessary.

Instrument Operation. Instrument operation is quite simple. When the instrument is turned on, both D_1 and D_2 (light-emitting diodes mounted on the front panel) are generally activated. Dry air is pumped through the hygrometer chamber, and the "clear" button is depressed a number of times. When the hygrometer output is brought below both set points, the lights go out. The instrument is now ready for measurement. At this point the "reset" button is depressed which clears the counters to zero. The humidity sensor is then placed on the leaf.

As the output from the sensor increases to the first set point, Q_2 fires and D_1 lights. At this point, the final control gate is opened, and the counter begins functioning. As the second set point is reached, Q_4 fires, D_2 lights, and the final control gate closes. The counters then cease functioning, and the final count is stored in the output. When the "display enable" button is depressed, the elapsed time between the two set points appears in the four-digit display. The prototype was built to count to 99.99 sec and automatically start over.

PARTS LIST

R_1: 2K trimpot
R_2: 200K 1%
R_3: 1.5K
R_4: 10K potentiometer
R_5, R_7, R_9, R_{12}, R_{14}: 1K
R_6, R_{10}, R_{11}, R_{15}, R_{20}: 4.7K
R_8, R_{13}: 5K trimpot
R_{16}: 10M
R_{17}: 10K
R_{18}: 15K
R_{19}: 100K
C_1(Osc.): 15 pf
C_1(Hum), C_3: 1μf
C_2: 0.1 μf
D_1, D_2: light-emitting diode
D_3, D_4: 1N914
Q_1: 2N3946, NPN, can be freely substituted
Q_2, Q_4: 2N2646, UJT, G.E.
Q_3, Q_5: HEP320, SCR, Motorola
1C-1, 1C-7: μA741, Signetics
1C-2, 1C-3: CD4001A, Quad 2-input nor gate, RCA
1C-4, 1C-5, 1C-6: DM74L90, low power decade scalers
1C-8: NE555, Signetics timer
x-tal: 100 kHz quartz crystal
CD4033A: Decade counter, seven-segment output type, RCA
CA3082: transistor array, RCA
Display: Shelly 3015F-CN low current seven-segment type
Batteries: (1) F4BP, 6V Burgess dry cell battery; (2) 2U6, 9V Burgess transistor battery

LITERATURE CITED

1. ALVIM, P. DE T. 1965. A new type of porometer for measuring stomatal opening and its use in irrigation studies. Arid Zone Res. 25: 325-329.
2. KANEMASU, E. T., G. W. THURTELL, AND C. B. TANNER. 1969. Design, calibration, and field use of a stomatal diffusion porometer. Plant Physiol. 44: 881-885.
3. KENNY, P. AND P. J. MCGRUDDY. 1972. A circuit for a self-timing stomatal diffusion porometer. Agr. Meteorol. 10: 393-399.